Wire-grid diffraction gratings used as polarizing beam splitter for visible light and applied in liquid crystal on silicon

M. Xu[1,2], H.P. Urbach[1,2], D.K.G de Boer[1], and H.J. Cornelissen[1]

[1] *Philips Research Laboratory*
Professor Holstlaan 4, 5656 AA Eindhoven, The Netherlands
[2] *Optics Research Group, Delft University of Technology*
Lorentzweg 1, 2628 CJ Delft, The Netherlands

Abstract: The application of wire grid polarizers as efficient polarizing beam splitters for visible light is studied. The large differences between the transmissivity for different polarizations are explained qualitatively by using the theory of metallic wave guides. The results of rigorous calculations obtained by using the finite element method are compared with experiments for both classical and conical mount. Furthermore the application of wire-grid polarizers in liquid crystal on silicon display systems is considered.

OCIS codes: (050.2770) Gratings; (230.1360) Beam splitters; (230.3720) Liquid-Crystal devices (120.5700) Reflection; (120.7000) Transmission; (160.3900) Metals; (230.5440) Polarization-sensitive devices.

References and links

1. Clark Pentico, Eric Gardner, Douglas Hansen, Ray Perkins, "New, high performance, durable polarizers for projection displays," SID 01 Digest 1287-1289 (2001).
2. E. Hecht, *Optics*, (Addison-Wesley Longman, New York, 1998).
3. X.J. Yu and H.S. Kwok, "Optical wire-grid polarizers at oblique angles of incidence," J. Appl. Phys. **93**, 4407-4412 (2003).
4. J. Chandezon, D. Maystre, and G. Raoult, "A new theoretical method for diffraction gratings and its numerical application," J. Opt. **11**, 235-241 (1985).
5. L. Li, "Multilayer diffraction gratings: differential method of Chandezon et al. revisited," J. Opt. Soc. Am. A **11**, 2816-2828 (1994).
6. M.G. Moharam and T.K. Gaylord, "Diffraction analysis of dielectric surface-relief gratings," J. Opt. Soc. Am. A **72**, 1385-1392 (1982).
7. J.B. Judkins and R.W. Ziolkovski, "Finite-difference time-domain modeling of nonperfectly conduction metallic thinfilm gratings," J. Opt. Soc. Am. A **12**, 1974-1983 (1995).
8. H.P. Urbach, "Convergence of the Galerkin method for two-dimensional electromagnetic problems," SIAM J. Numer. Anal. **28**, 697-710 (1991).
9. L. Li, "A modal analysis of lamellar diffraction gratings in conical mountings," J. Mod. Opt. **40**, 553-573 (1993).
10. H. Raether, *Surface Plasmons on Smooth and Rough Surfaces and on Gratings*, (Springer-Verlag, Berlin, 1988).
11. J.M. Brok and H.P. Urbach, "Rigorous model of the scattering of a focused spot by a grating and its application in optical recording," J. Opt. Soc. Am. A **2**, 256-272 (2003).
12. J.D. Jackson, *Classical Electrodynamics*, (John Wiley & Sons, Inc., U.S. 1975).
13. Stephen Arnold, Eric Gardner, Douglas Hansen, and Ray Perkins, "An Improved Polarizing Beamsplitter LCOS Projection Display Based on Wire-Grid Polarizers," SID 01 Digest, 1282-1285 (2001).
14. http://www.autronic-melchers.com
15. E.Palik and G.Ghosh, *Handbook of optical constants of solids*, (Academic Press, New York, 1998).
16. Pochi Yeh and Claire Gu, *Optics of Liquide Crystal Displays*, (John Wiley & Sons, Inc., New York, 1999).

#6733 - $15.00 US Received 1 March 2005; revised 14 March 2005; accepted 15 March 2005

17. Pochi Yeh, "Generalized model for wire grid polarizers," in *Polarizers and Applications*, Giorgio B. Trapani. Bellingham, eds., Proc. SPIE **307**, 13-21 (1981).

1. Introduction

The wire-grid polarizer (WGP) is a metallic grating with period smaller than the wavelengths for which it is used. An example is shown in Fig. 1. Let a plane wave be incident on the grating. We assume first that the wave vector of the incident plane wave is in the plane perpendicular to the grooves. This case will be called the *classical mount*. According to our coordinate system (see Fig. 2), $\phi = 90^\circ$ for this case. When the incident light is linearly polarized such that the electric vector is parallel to the wires (or grooves) of the WGP, the light is almost totally reflected as if the WGP were a flat metallic mirror. This state of polarization is called s-polarization because the electric field is perpendicular (Senkrecht) to the plane of incidence through the incident wave vector and the z-axis in Fig. 1. When the incident light is linearly polarized such that the electric field is perpendicular to the wires, most of the light is transmitted. This state of polarization is called p-polarization because the electric vector is parallel to the plane of incidence. It follows that when the incident light is unpolarized, the reflected light is predominantly s-polarized whereas the transmitted light is predominantly p-polarized. The WGP can thus be used as a polarizer. As such it is well known in applications in the infrared part of the spectrum. Using advances in nano fabrication technology, periodic metallic gratings with periods smaller than the wavelength are now finding applications in optics. A WGP has higher contrast and is less expensive than a conventional MacNeille polarizing beam splitter (PBS) based on thin layers on prismatic glass. Therefore, a WGP is a good alternative PBS in many applications such as projection systems in liquid crystal on silicon (LCoS) displays [1]. When the wave vector of the incident plane wave is not in the plane perpendicular to the grooves, i.e. ϕ is arbitrary. This case will be called the *conical mount* as shown in Fig. 2(b). In this case, the s- and p-polarizations are coupled then the grating can not be used as a beam splitter.

Because plasmon resonance surface waves can be excited by a p-polarized incident plane wave whereas for s-polarization these waves never occur, one might think that plasmons can explain the working of a WGP. We shall show however that, at least for the WGP studied in this paper, plasmons are not excited. A common explanation of the WGP is based on the restricted

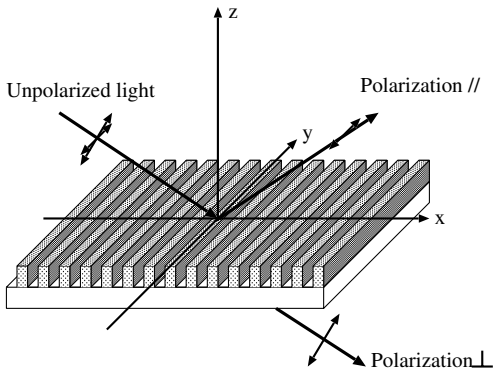

Fig. 1. An example of a WGP. When unpolarized light incident on the polarizer, polarization with electric field parallel to wire grid is reflected and polarization with electric field perpendicular to the wire grid is transmitted.

#6733 - $15.00 US Received 1 March 2005; revised 14 March 2005; accepted 15 March 2005

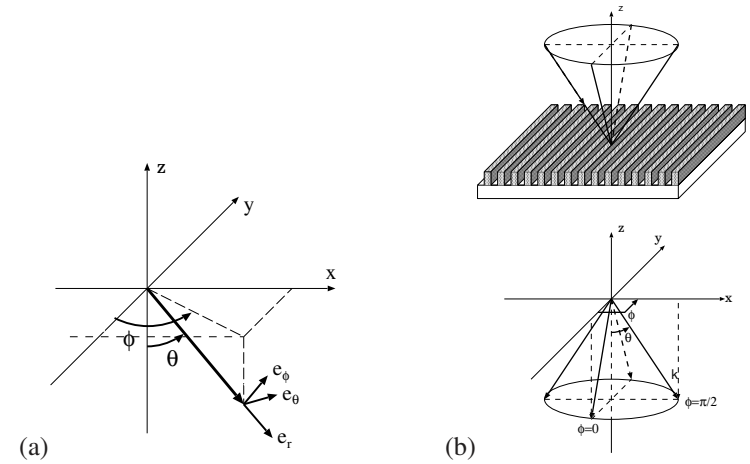

Fig. 2. (a) Coordinate system. (b) Cone of incident rays with respect to normal of the WGP surface.

movement of electrons perpendicular to the metal wires (see [2] and [3]). In Section 2.1, we present a new qualitative explanation. We show that by considering one cell of the grating as part of a rectangular metallic wave guide, the large differences in transmission between the polarizations can be explained by the differences between the propagation constants of the guided modes for the two polarizations.

In Section 3 we describe the rigorous model and the experimental set-up that we used for the quantitative analysis of WGPs. Several rigorous computational methods exist for diffraction gratings, e.g. those described in [4], [5], [6] and [7]. Some of these were at least initially developed for classical mount and extension to conical mount is not always straightforward. We used a model based on the finite element method (FEM) which has been described in [8]. The FEM is a general numerical method for solving boundary value problems. A lot is known about the mathematical properties of this method so that it can be applied with confidence. The main reason for us to use this method is that all kinds of geometries and materials can be simulated. Furthermore, the conical incident angles are not more difficult to solve than the classical mount. The model furthermore has the advantage over e.g. FDTD (finite difference time-domain) [7] that the radiation conditions that are implemented are not of absorbing type and hence approximative, but instead are exact. In a recent paper [3], Yu and Kwok have studied the WGP in optics by applying the rigorous modal method developed by Li [9] to study the dependence on the polar angle in classical mount. The case of conical mount is much more difficult to solve with this method than the classical mount. Indeed, in [3] the only case of conical mount considered is that for which the incident wave vector is parallel to the grooves and in that case a simplified model is used. In contrast, we study the case of conical mount also for other angles of incidence. As stated above, for the FEM the conical case is not more difficult than classical mount. The case of polar angle of 45° is very important for the application in liquid crystal on silicon(LCoS) systems that is considered in Section 5. The theoretical and experimental results that we present in Section 4 demonstrate that also for polar angle of 45° and for azimuthal angles in the range $-15^\circ < \phi < 15^\circ$, the WGP is surprisingly efficient.

#6733 - $15.00 US Received 1 March 2005; revised 14 March 2005; accepted 15 March 2005

2. Qualitative analysis

2.1. Plasmons

Along an interface between a dielectric and a metal of which the real part of the permittivity is negative, a surface wave can propagate. When the z-axis is normal to the interface, the wave vector of the plasmon wave inside the dielectric is given by [10], [11]:

$$\mathbf{k}^{pl} = (k_x^{pl}, k_y^{pl}, k_z^{pl}), \tag{1}$$

with approximately

$$(k_x^{pl})^2 + (k_y^{pl})^2 \equiv (k_{\|}^{pl})^2 \gtrapprox k_0^2 n^2, \tag{2}$$

where n is the refractive index of the dielectric and k_0 is the wave number in a vacuum. In fact, k_x and k_y have small but nonzero imaginary part, hence the wave is slowly damped as in propagates along the surface. The magnetic field of the plasmon wave is perpendicular to the plane through the z-axis and the real part of the vector $(k_x^{pl}, k_y^{pl}, 0)$, hence the wave is p-polarized. Now let $\mathbf{k} = (k_x, k_y, k_z)$ be the wave vector of a p-polarized wave that is incident on the WGP. The wave vector corresponding to the mth reflected order is:

$$(k_x + \frac{2\pi m}{p}, k_y, k_z^m), \tag{3}$$

where $k_z^m = \left[k_0^2 n^2 - (k_x + \frac{2\pi m}{p})^2 - (k_y)^2\right]^{1/2}$. This wave corresponds can excite a surface plasmon when there holds

$$(k_x + \frac{2\pi m}{p})^2 + (k_y)^2 \approx (k_{\|}^{pl})^2. \tag{4}$$

The WGPs that we study in this paper have period considerably smaller than $\lambda/2$ with λ the wavelength in the dielectric. Therefore we have that $2\pi/p$ is considerably larger than $k_0 n$. Hence (4) can never be satisfied for an integer m. Hence plasmon resonances are not responsible for the large differences between the polarizations.

2.2. Metallic waveguide theory

In this section we consider one cell of the grating as part of a metallic grating [12] and study the guided modes in such a waveguide to explain the performance of the WGP *qualitatively*. The field in such a guide can be written as a linear superposition of so-called waveguide modes. In this section we shall only consider electromagnetic fields that are independent of y.

Suppose we have a two dimensional infinitely long slab waveguide, as shown in Fig. 3. The regions I and III with refractive index n_1 consist of the same metal. The medium in region II is homogeneous dielectric with real refractive index n_0. The width of the middle region is w. Then we can write the index of refraction as:

$$n = \begin{cases} n_0, & -w/2 < x < w/2, \\ n_1, & |x| \geq w/2. \end{cases} \tag{5}$$

A waveguide mode is a field that depends on z by a factor $\exp(\pm i\beta z)$, where β is the so-called propagation constant. We will consider only modes that are independent of y. There are two types of modes, namely TE modes of which the electric field is parallel to the y-direction and TM modes of which the magnetic field is parallel to the y-direction.

There are infinitely many in general complex values for the propagation constants which differ for TE and TM modes. When the material in region I and III is a perfect conductor, the

#6733 - $15.00 US Received 1 March 2005; revised 14 March 2005; accepted 15 March 2005

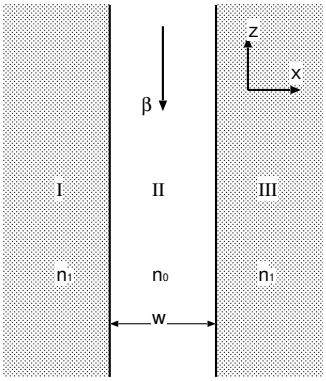

Fig. 3. Infinitely long slab waveguide, independent of y-axis.

following holds [12]

$$\beta_m = \sqrt{k_0^2 n_0^2 - \frac{m^2\pi^2}{w^2}},\ m = 1,2,3,\ldots \text{ For TE modes,} \tag{6}$$

$$\beta_1 = k_0 n_0, \beta_m = \sqrt{k_0^2 n_0^2 - \frac{(m-1)^2\pi^2}{w^2}},\ m = 1,2,3,\ldots \text{ For TM modes.} \tag{7}$$

Note that these numbers are either real or purely imaginary and that when $w < \lambda/(2n_0)$ all β_m are purely imaginary in the TE case. Then the amplitudes of all TE-polarized modes decrease exponentially with z. In contrast, for TM there is always at least one real propagation constant, namely $\beta_1 = k_0 n_0$, no matter how small w is.

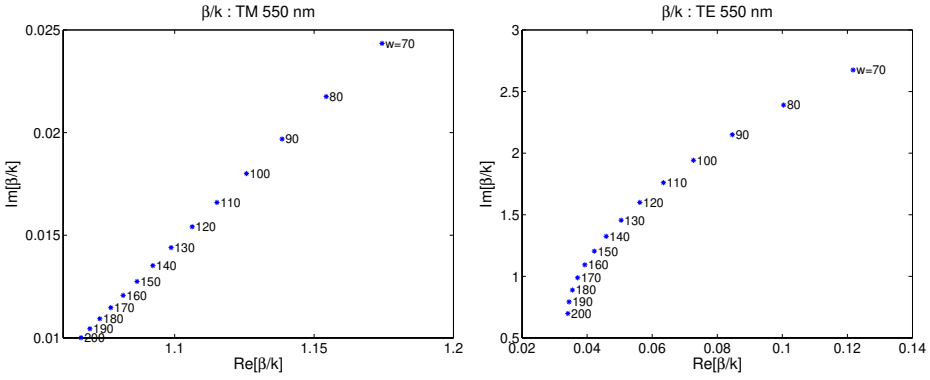

Fig. 4. Propagation constant of the lowest TE and TM modes in the complex plane as function of the width of the groove. The wavelength of the incident light is 550 nm. Left is TM polarization, and right is TE polarization. The axes are normalized by the wave number in vacuum.

When the finite conductivity of the metal is taken into account, the propagation constants all have non-vanishing imaginary part.In Fig. 4 the propagation constants β for aluminum are shown for a set of values of the width w. The wavelength in the dielectric is 550 nm. It is seen

#6733 - $15.00 US
Received 1 March 2005; revised 14 March 2005; accepted 15 March 2005

that when $w < \lambda/2n_0$ the propagation constant β_1 of Al for TE is always close to the imaginary axis whereas for TM the β_1 is close to the real axis.

Let an s-polarized plane wave whose wave vector is in the plane perpendicular to the grooves, be incident on a WGP. Such an incident field excites only TE-modes in the guide. For the WGPs it holds that $w < \lambda/2n_0$, hence the propagation constants of all TE-modes have large imaginary parts. The amplitude of the transmitted field is thus exponentially smaller than that of the incident field. Conversely, when the incident plane wave is p-polarized (again with wave vector in the plane perpendicular to the grooves), its magnetic field is parallel to the grooves and hence only the TM modes are excited in the guides. Since the fundamental mode has a propagation constant with only a small imaginary part, a large fraction of the incident energy is transmitted. This explains qualitatively the working of a WGP.

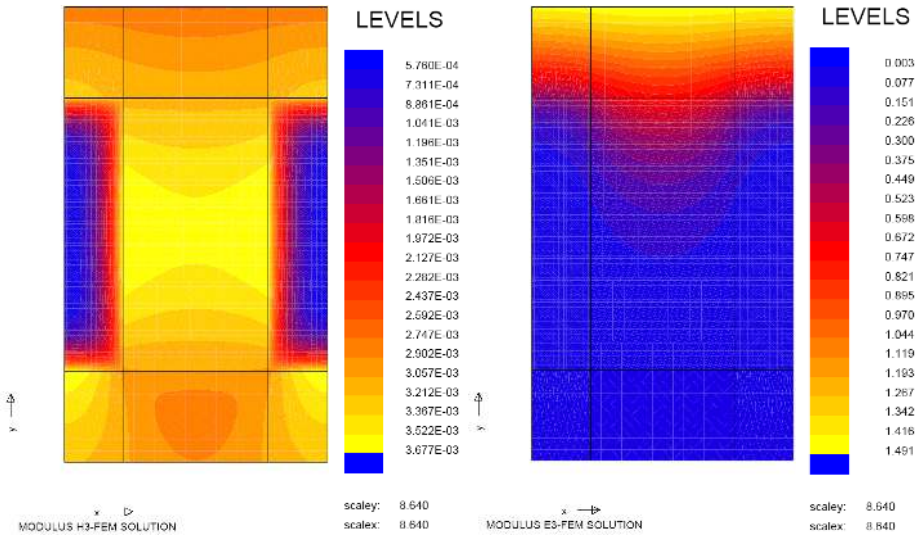

Fig. 5. Field in unit cell at normal incidence for green light (with wavelength of 550 nm). At the left the field is s-polarized and the amplitude of the electric field component along the grooves is shown. At the right the field is p-polarized and the amplitude of the magnetic field component parallel to the grooves is shown. The field has been calculated by the rigorous finite element model described in Section 3.1. (Note that the y-axis in these figures is called the z-axis in Fig. 1).

As an example we show in Fig. 5 the electromagnetic fields inside one period of the WGP when the incident light has wavelength $\lambda = 550$ nm, the period $p = 144$ nm and the duty cycle $D = 45\%$. The perpendicular incident plane wave is either s- or p-polarized. The field in one cell of the grating was calculated rigorously by using the rigorous finite element method with periodic boundary conditions imposed as described in Section 3.1. It is seen that the total field is strongly evanescent in the case of s-polarization, but propagates through the groove in the case of p-polarization.

3. Computational model and experimental procedure

3.1. Computational model of a wire-grid grating

One could in principle use the waveguide model to calculate the electromagnetic field rigorously in the grating. However, this would require that the coupling efficiencies between the

#6733 - $15.00 US
Received 1 March 2005; revised 14 March 2005; accepted 15 March 2005

incident field and the waveguide modes are determined. Furthermore, the waveguide model would be difficult to apply to V-shaped grooves. We therefore decided to use the FEM for rigorous quantitative analysis. An advantage of the FEM model is that the case of conical incidence is not more difficult than the classical case.

For details about the method based on the FEM and its application to diffraction gratings we refer to [8] and [11]. Here we only give a general description.

Consider a one-dimensional periodic diffraction grating as shown in Fig. 1. With respect to the coordinate system (x,y,z) the grating is periodic in the x-direction and is translational invariant in the y-direction. In such a configuration there are solutions of Maxwell's equations of the form

$$\begin{aligned} \mathbf{E}(\mathbf{r},t) &= \mathbf{U}(x,z)\, e^{i(k_y y-\omega t)}, \\ \mathbf{H}(\mathbf{r},t) &= \mathbf{V}(x,z)\, e^{i(k_y y-\omega t)}, \end{aligned}$$

for some numbers ω and k_y and for some vector fields $\mathbf{U}$ and $\mathbf{V}$ that are periodic in x apart from a common phase shift. It can be shown that for given ω and k_y Maxwell's equations are equivalent to a system of two coupled second order partial differential equations for only the components E_y and H_y. When we consider the scattering of an incident plane wave in classical mount, we have $k_y = 0$. Then the two partial differential equations for E_y and H_y are uncoupled (one contains only E_y, the other only H_y) and when the incident plane wave is s- or p-polarized, the same is true for the total field. In conical mount however, there holds $k_y \neq 0$. Then the two partial differential equations are coupled and the polarizations mix. Hence, when the incident wave is s- or p-polarized, the total field is to some degree elliptically polarized. It is thus seen that the formulation in terms of the system of two, in general coupled, partial differential equations for E_y and H_y is valid for the general conical case and that the classical mount is only a special case of the general formulation.

One can derive a boundary value problem for the system of two partial differential equations on a rectangular region Ω in the cross-sectional plane $y = 0$ which has width of one period in the x-direction and is so large in the z-direction that above and below Ω there are homogeneous half spaces. The boundary values for E_y and H_y on the boundaries $x =$ constant are derived from the periodicity of the tangential electric and magnetic field components. The boundary values on the boundaries $z =$ constant are derived by using plane wave expansions for the field in the half spaces above and below Ω. A non-local boundary condition is obtained which expresses the tangential magnetic field in terms of the tangential electric field components by means of a pseudo-differential operator. This boundary condition is rigorous in the sense that the boundary value problem on Ω is completely equivalent to the original scattering problem for Maxwell's equations. It differs in this respect markedly from for instance approximative absorbing boundary conditions that are often used in other methods such as FDTD.

The solution of the boundary value problem on Ω is computed by using the finite element method (FEM). This is a general mathematical method for solving all kinds of boundary value problems. It is very flexible regarding changing geometries and materials (for example metals and large optical contrast do no cause any problems). Furthermore, a lot of properties of the FEM have been proved mathematically. We stress that the method based on the FEM that we have used and that used by [3] as developed by Li[5] are both rigorous but that they otherwise are totally different.

3.2. Experiment

The WGP samples have been obtained from Moxtek Inc [13]. Measurements of transmission and reflection of the WGP at the classical mount and reflection at the conical mount have been done. An *autronic-MELCHERS* detector [14] which can measure the intensity of the emitted

#6733 - $15.00 US Received 1 March 2005; revised 14 March 2005; accepted 15 March 2005

light as function of wavelength was used in the experiments. The same detector is used to measure the incident light intensity and the reflected and transmitted light. A diffusive white light source is used for transmission measurements. For reflection measurements, collimated light is used.

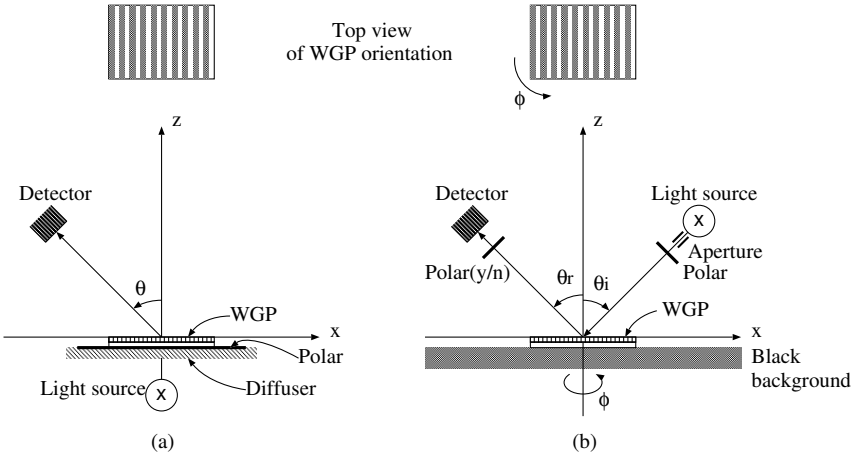

Fig. 6. Set up for measurement of transmission (a) and reflection (b).

Figure 6 shows the simplified arrangement for the measurements. For classical mount, the WGP is positioned vertically and the wire grid front always faces the light source, that is, the transmission takes place at the glass front and reflection at metal wires front. A sheet polarizer is mounted on the light source with vertical or horizontal position to obtain a s- or p-polarized incident beam. In transmission experiments, the detector moves in the plane perpendicular to the wire-grid with θ changing from 25° to 65° in steps of 5° in order to measure the transmitted light at those angles. For reflection measurements, the light source and the detector are aligned in the plane perpendicular to the wire-grid. The angles θ_i and θ_r in Fig. 6(b) are the same and are varied between 25° to 65° in steps of 5°. In this way, the reflected intensity is obtained.

For arbitrary conical incident angles, we have measured the reflected intensity. In this case, the wire grid front faces the light source and detector, i.e. reflection takes place at the aluminum wire grid front. The light source and detector are fixed at $\theta_i = \theta_r = 45°$, and the basis table rotates for varying conical angles from $\phi = 90°$ to $\phi = 0°$. Because at the conical mount, the scattered field is not purely s- or p-polarized, but instead a mixture of the two. There is an other polarizer used in front of the detector in order to measure separately the s- or p-polarized components of the reflected light.

4. Results

4.1. General cases

4.1.1. The Influence of the Depth of the Groove

In Fig. 7 the calculated depth dependence of wire grid performance for 550 nm incident radiation at classical mount ($\phi = 90°$) is shown. The duty cycle has been chosen equal to 45%, hence, because the period was 144 nm, the width of the wires was 65 nm. The depth of the wires varies between 10 nm and 400 nm. The green curves in the figures are for normal incidence at $\theta = 0°$ and the blue curves correspond to oblique incidence at $\theta = 45°$.

#6733 - $15.00 US Received 1 March 2005; revised 14 March 2005; accepted 15 March 2005

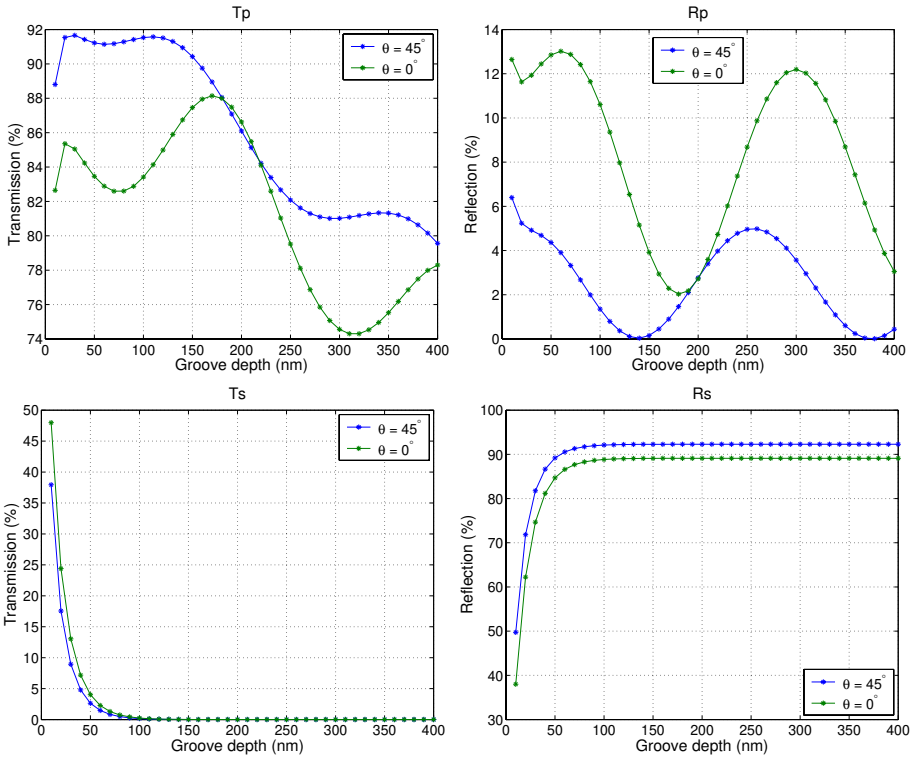

Fig. 7. Reflection and transmission for 550 nm wavelength at classical mount ($\phi = 90^\circ$) as functions of the depths of the grooves. Green line: normal incidence ($\theta = 0^\circ$). Blue line: oblique incidence ($\theta = 45^\circ$). Tp and Ts are the transmitted intensities for p- and s-polarization in the z-direction, respectively. Rp and Rs are the reflected intensities for p- and s-polarization in the z-direction respectively.

The data show that the case of 45° incidence gives better performance, i.e. higher p-polarization transmission and s-polarization reflection and lower p-polarization reflection and s-polarization transmission. Meanwhile the performance depends strongly on the polarizations. For s-polarization, at both normal and oblique incidence, the reflection and transmission become almost constants after the wires depth is increased to 100 nm. For p-polarization, the performance is periodic because of the phase interference. For p-polarized light at normal incidence (green lines in the figures), the transmission of p-polarized light peaks at depth 170 nm corresponding to the lowest reflection. At oblique incident angle of 45°, the transmission of p-polarization peaks at $110 \sim 130$ nm while the reflection of p-polarization approaches almost zero at $140 \sim 150$ nm, which corresponds to a quarter wavelength. When the depth is in this range, we get better polarization efficiency. In the following simulations, the depth of the wires was set equal to 150 nm.

4.1.2. Classical mount

The geometry of the WGP is described by the following parameters: period p=144 nm, depth of the wires d=150 nm, and width of the groove w=79 nm. A picture of the WGP obtained by using a scanning electron microscope (SEM) is shown in Fig. 8. For the case that the plane of incidence is perpendicular to the grooves (classical mount), the calculated and measured

#6733 - $15.00 US Received 1 March 2005; revised 14 March 2005; accepted 15 March 2005

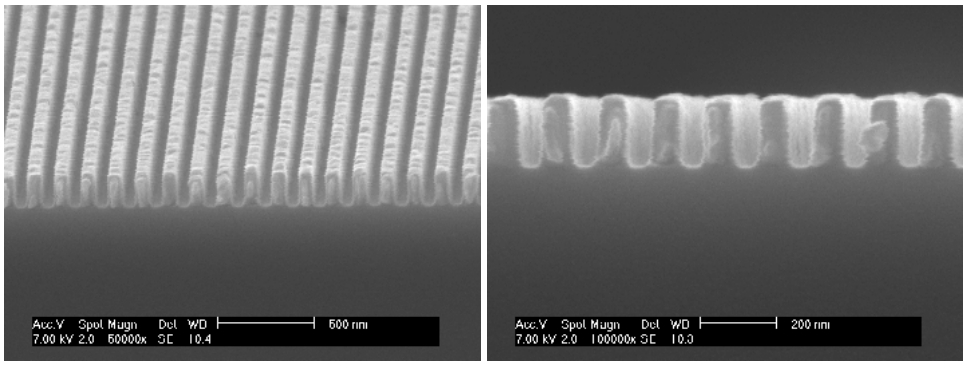

Fig. 8. SEM photos of a WGP sample.

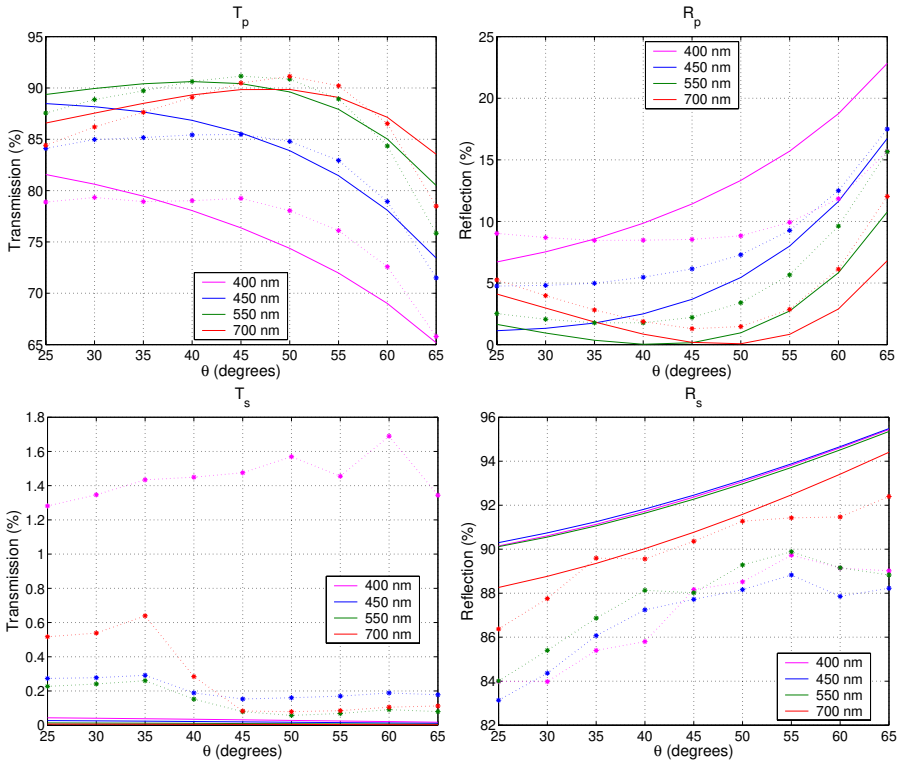

Fig. 9. Comparison between simulated (solid line) and measured (star-dotted line) reflected and transmitted intensities for classical mount ($\phi = 90^\circ$) as function of θ. The light is incident from the wire grid side. Thus for transmitted measurements, the glass side faces the detector, and for reflected measurements, the wire grid side faces the detector.

dependence on the polar angle θ are shown in Fig. 9.

It can be seen that in general the experimental and simulated results are similar. For p-polarization the agreement is quite good. For the case of transmission of s-polarization, the intensity received by the detector is so low that the detected signals are strongly affected by

#6733 - $15.00 US Received 1 March 2005; revised 14 March 2005; accepted 15 March 2005

noise. For a more stable environment and longer exposure times, the measured data are expected to be lower. Small geometric differences can affect the performance of the WGP.

4.1.3. Metals

Different metals have different refractive indices, which affect the performance much. We consider now two other metals, gold and silver.

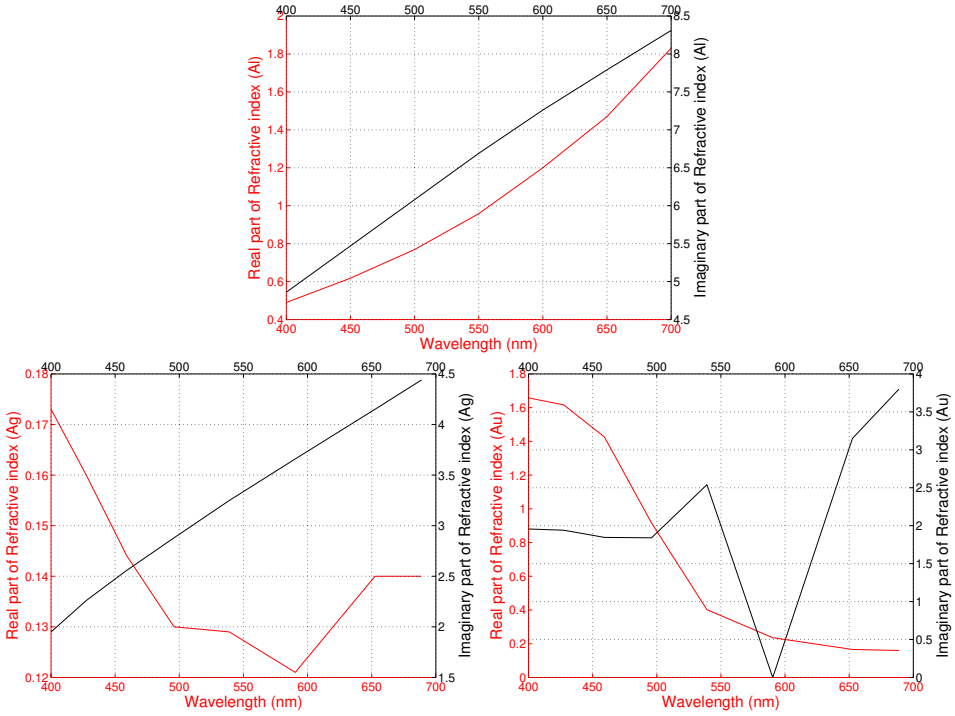

Fig. 10. Real (red curve) and imaginary part (black curve) of the refractive index of aluminum (top), silver (left bottom) and gold (right bottom) as function of wavelength in the range of visible light.

The refractive indices [15] of aluminum, gold, and silver are shown in Fig. 10 as functions of wavelength. Red curves denote the real part and black ones the imaginary part. It is seen that both the real and imaginary part of refractive index of aluminum are nearly linearly increasing with wavelength in the range of visible light. At classical mount, with the polar angle θ fixed at 45°, the simulated reflection and transmission as function of incident wavelength for the gratings of different metals is shown in Fig. 11. It is seen in Fig. 11 that the WGP of aluminum is better than that of gold and silver. The contrast ratios of transmission and reflection are much larger for Al than for the other two metals. In general, metals with refractive indices with larger imaginary and smaller real part give better results.

4.1.4. Conical mount

When the plane of incidence is not perpendicular to the wire grids the field is said to be at *conical mount* (see Fig. 2). In this case, s- and p-polarizations are coupled, when the incident field is s- or p-polarized, the transmitted or reflected field is not purely s- or p-polarized. We consider the reflected and transmitted intensities for varying azimuthal angle ϕ.

#6733 - $15.00 US Received 1 March 2005; revised 14 March 2005; accepted 15 March 2005

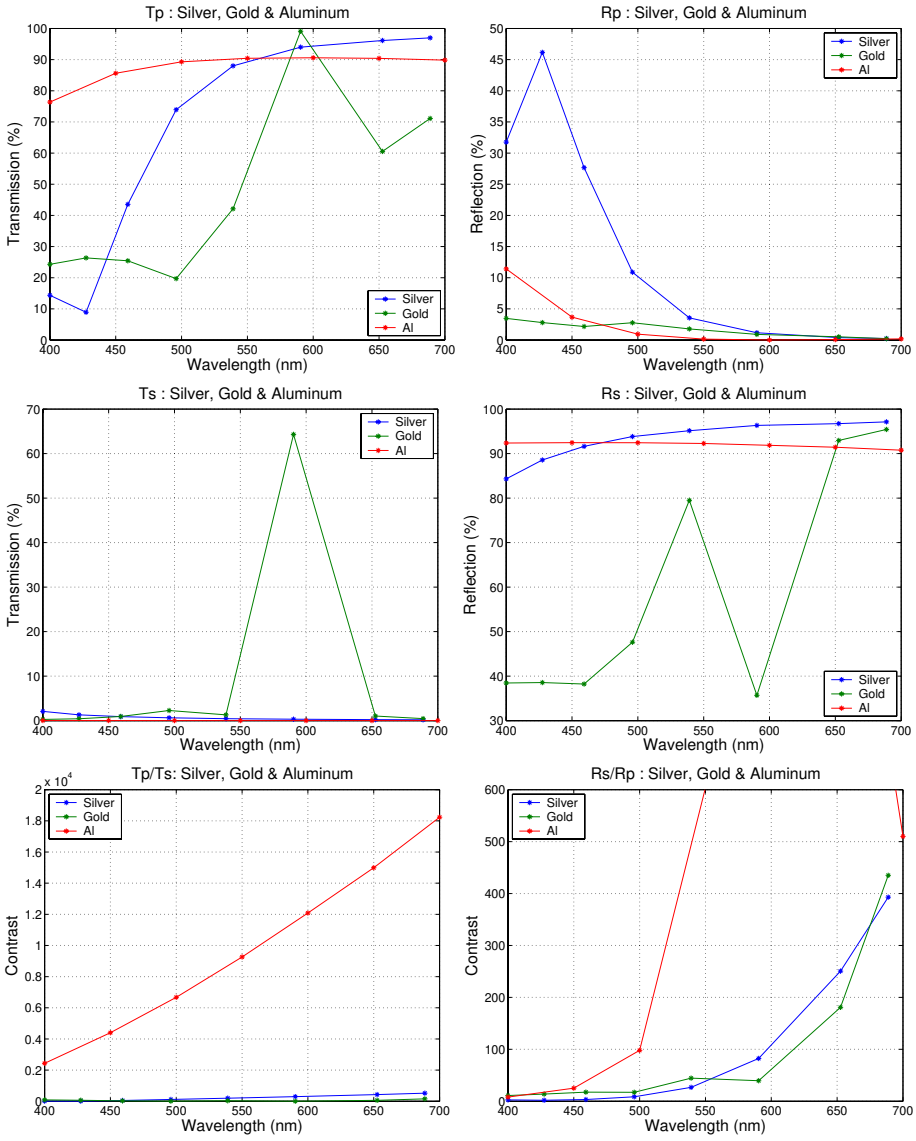

Fig. 11. Performance of three metals at classical mount, $\theta = 45^\circ$ and $\phi = 90^\circ$, as function of wavelength.

#6733 - $15.00 US
Received 1 March 2005; revised 14 March 2005; accepted 15 March 2005

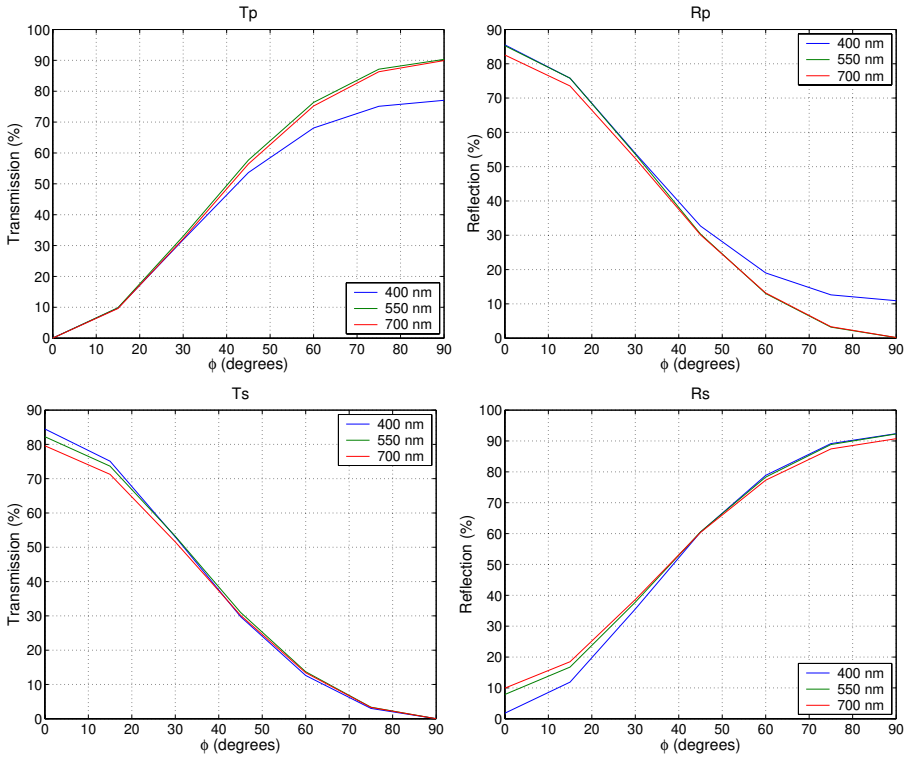

Fig. 12. Conical incident angle with respect to normal at $\theta = 45^\circ$.

The polar angle θ is kept at 45° while the azimuthal angle ϕ is varied from 0° to 90° in steps of 15°. The incident rays are thus on a cone with its axis normal to the surface as depicted in Fig. 2. The simulated results for the transmission and reflection coefficients as function of ϕ are plotted in Fig. 12. The transmission of p-polarized light drops as ϕ is reduced from 90° to 0°, while the transmission of the s-polarization increases as expected. The reflection coefficients behave similarly. When ϕ decreases, the reflection of s-polarized light decreases and that of p-polarized light increases.

When the plane of incidence is perpendicular to the wire grids, i.e. at classical mount ($\phi = 90^\circ$), the electric field of p-polarization is perpendicular to the wire grids. When the plane of incidence is parallel to the wire grids ($\phi = 0^\circ$), the electric field of p-polarization is not perpendicular to the wire grids. In this position the electric field of p-polarized light has a y-component which is in the direction parallel to the wire grids and this results in a high reflection of p-polarization at this position.

When the plane of incidence is not at classical mount, the polarizations get coupled. The polarization states [16] of the light are then not any more linear, but elliptic. In Fig. 13, the polarization states are shown as function of ϕ for wavelength of 550 nm. The *polar angle* θ along the vertical axis is the propagation direction after scattering.

In the case of pure s-polarization, the electric field is in the direction of the ϕ-axis. In the case of p-polarization, the electric field is along the θ-direction. We can see in Fig. 13 that at the classical mount of $\phi = 90^\circ$ and at the special conical mount of $\phi = 0^\circ$, the polarization states of the transmitted and reflected fields are the same as that of the incident field, i.e. they are

#6733 - $15.00 US
Received 1 March 2005; revised 14 March 2005; accepted 15 March 2005

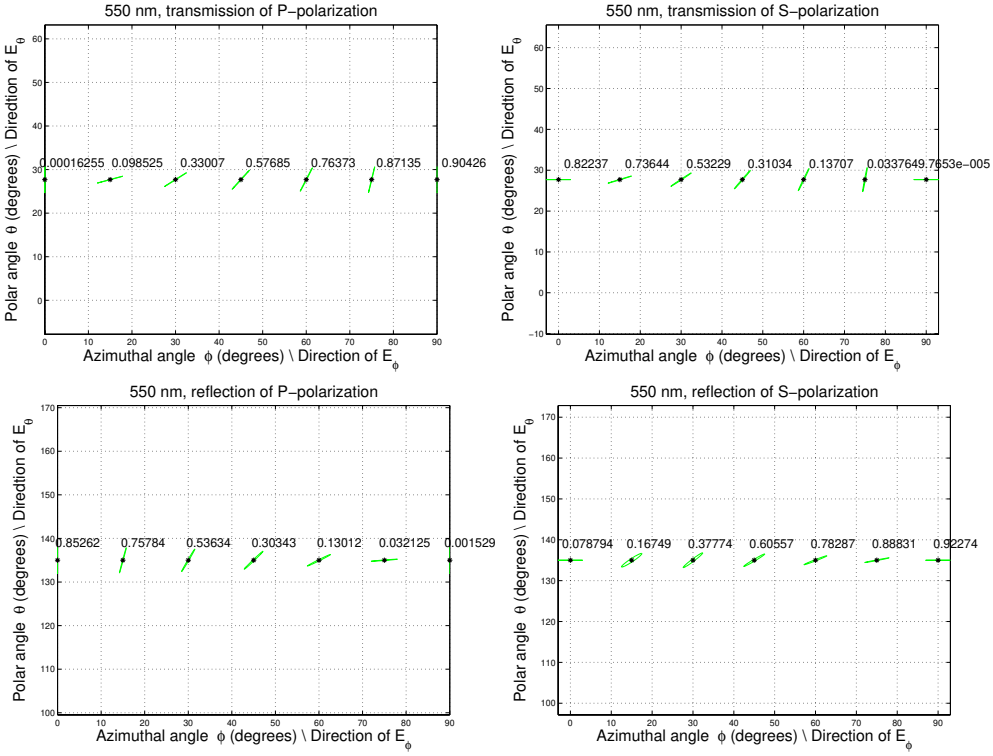

Fig. 13. Polarization states for 550 nm wavelength as function of angle ϕ ($0 \leq \phi \leq 90^\circ$) and for $\theta = 45^\circ$. The ϕ-axis is also the direction of E_ϕ and the vertical axis is also the direction of E_θ.

purely s- or p-polarized. The polarization states for the cases $0 < \phi < 90^\circ$ are elliptic with small ellipticity and a mix of s- and p-polarized signals. The ellipticity is important and hampers a good contrast. Furthermore, the numbers marked around the ellipses denote the total intensity of the transmitted or reflected light. At $\phi = 0^\circ$ for s-polarization, although the transmitted and reflected field are also s-polarized, most of the light is transmitted while it is mostly reflected at $\phi = 90^\circ$.

The elliptically polarized reflected and transmitted field can be decomposed as follows. When the incident field is s-polarized and has unit amplitude, R_{ps} denotes the amplitude of the p-polarized component of the reflected field. Similar definitions holds for R_{ss}, R_{sp} and R_{pp}. With the experimental set-up as shown in Fig. 6(b) these reflectivity components can be measured. The mounted polarizer on the detector in this conical experiment reduces the measured intensity significantly. The total reflected intensity at ($\phi = 90^\circ$) should equal the previous measurement taken at classical mount, i.e. $R_{ss} + R_{ps} = R_s$, hence the reduction ratio can be calculated and it is was found to be 64%. The comparison between measurements and simulations are shown in Fig. 14. The star-dotted computed lines are in good agreement with the measured solid lines.

In Fig. 15 and Fig. 16 calculated results obtained by the rigorous diffraction method and the effective medium method [17] are compared as functions of the azimuthal angle ϕ at polar angle $\theta = 45^\circ$. Figure 15(a),(b) show the reflectivity and transmissivity components for incident s- and p-polarized light, respectively. Figure 16(a),(b) show the orientation of the polarization ellipse and the ellipticity of the reflected (R) and transmitted (T) light for the two polarizations

#6733 - $15.00 US Received 1 March 2005; revised 14 March 2005; accepted 15 March 2005

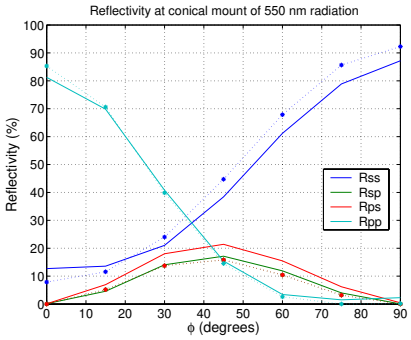

Fig. 14. Comparison between simulations (star-dotted lines) and measurements (solid lines) at conical mount with $\theta = 45^\circ$ for 550 nm wavelength incident radiation. The computed results of R_{sp} are overlapped by those of R_{ps}.

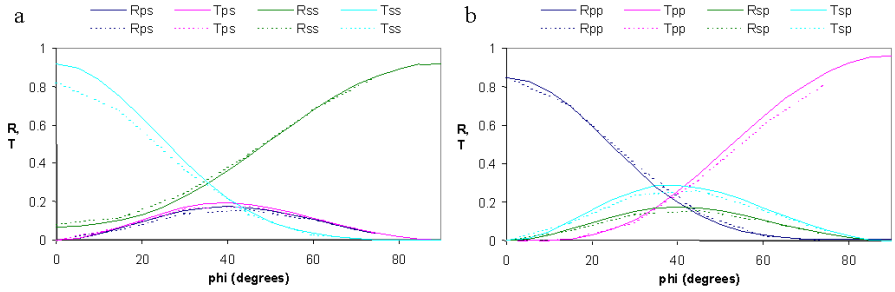

Fig. 15. Reflectivity and transmissivity of a WGP for incident s-polarized (a) and p-polarized (b) light at a wavelength of 550 nm and at $\theta = 45^\circ$ as functions of ϕ. Solid lines: calculated with Berreman's method and effective-medium theory. Dotted lines: calculated with rigorous diffraction theory (finite-element method).

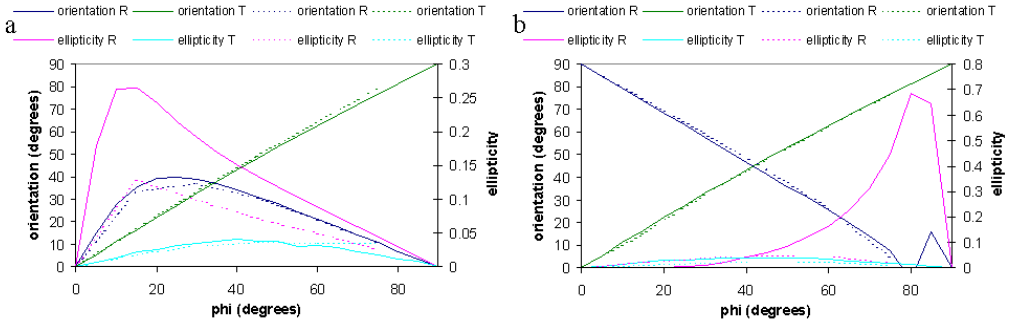

Fig. 16. Orientation of the polarization ellipse and the ellipticity defined in the text for incident s-polarized (a) and p-polarized light (b) at $\lambda = 500$ nm and $\theta = 45^\circ$ as a function of ϕ. Solid lines: calculated with Berremans method and effective-medium theory. Dotted lines: calculated with finite-element method.

#6733 - $15.00 US
Received 1 March 2005; revised 14 March 2005; accepted 15 March 2005

of incident light. The solid line are calculated with the effective medium method and the dotted lines are calculated with the rigorous diffraction method. As can be seen, the agreement between the results obtained by the two methods is rather good and within the margin between experiments and calculations. Only for the case of the ellipticity of the reflected light the agreement is bad. Note, however, that in that case the intensity of the reflected light is low.

5. Application in LCoS optical assemblage

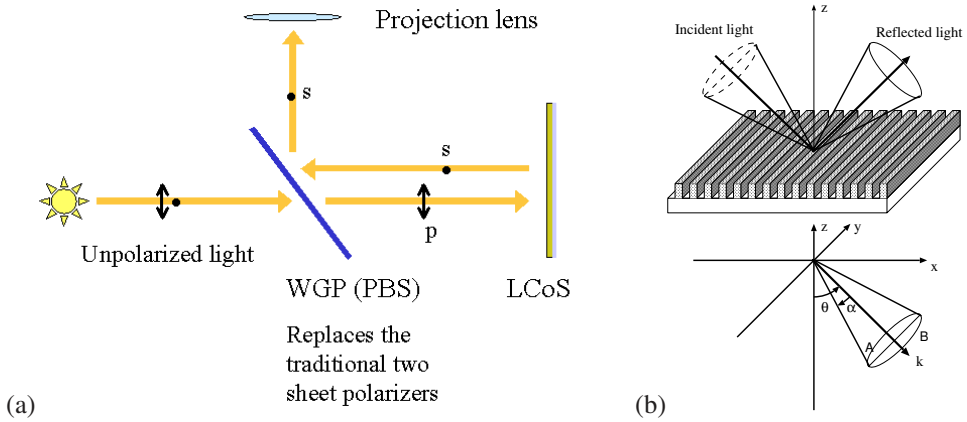

Fig. 17. (a) Single LCoS panel rear projection display.(b) A cone of incident rays with the chief incident ray of $\phi = 90^\circ, \theta = 45^\circ$ as axis of the cone.

The light path in a projection system of a liquid crystal display system is shown in Fig. 17(a). The liquid crystal is situated on a silicon substrate, therefore this set-up is called LCoS. The unpolarized light that is emitted by the light source is first collimated and is then incident on the WGP with angle of incidence of 45°. The light transmitted by the WGP and incident on the LCoS is thus predominantly p-polarized. When the LCoS panel rotates the polarization such that the light reflected by the silicon is s-polarized, the WGP reflects the light to the projector lens. Because in this application the light makes angle of 45° with the WGP, the polarizing behavior for in particular this angle of incidence is important. Because the light wave is not plane but instead consists of a cone of incident rays, the tolerance of the WGP for other angles of incidence must also be studied.

In the application assembly, the incident light is a cone of rays with center given by $\theta = 45^\circ, \phi = 90^\circ$ as shown in Fig. 17(b). For an F/2.0 pupil, the range of the angles of the cone would be from 30.5° to 59.5°. The cone of incident rays causes that the polarization of the reflected and the transmitted rays cannot be perfect.

Referring to Fig. 17(b), rays in the (x,z)-plane are in the classical mount, and hence s- and p-polarized states are separated. For other rays, the reflected and/or transmitted field will be a mixture of two polarizations. We define a plane Σ which is fixed by the wave vector $\mathbf{k}$ of the chief ray (at $\theta = 45^\circ$ and $\phi = 90^\circ$) and the y-axis. The angle of α is defined as the angle of an arbitrary ray deviating from the chief ray in the Σ-plane. With a ray moving away from the chief ray with angle α, the corresponding ϕ and θ are given by:

$$\phi = \arctan\left(\frac{\sqrt{2}}{2\tan\alpha}\right), \tag{8}$$

#6733 - $15.00 US
Received 1 March 2005; revised 14 March 2005; accepted 15 March 2005

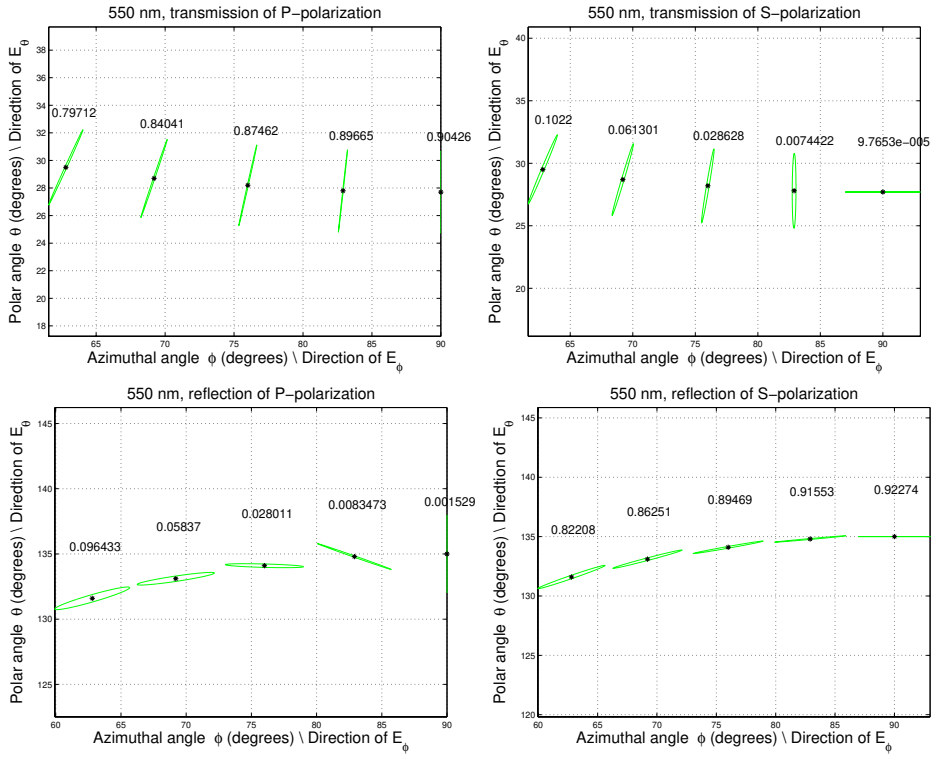

Fig. 18. Polarization states for 550 nm wavelength incident light for varying field angle α of the cone, with the chief ray at $\theta = 45^\circ$, $\phi = 90^\circ$. Numbers around the ellipses are the total reflectivity or transmissivity.

$$\theta \quad = \quad \arccos\left(\frac{\sqrt{2}\cos\alpha}{2}\right). \tag{9}$$

For $\alpha = 5^\circ, 10^\circ, 15^\circ$ and 20°, the corresponding values of ϕ and θ are listed in Table 1. For these cases, the states polarization of the reflected and transmitted field are shown in Fig. 18.

α	ϕ	θ
5	82.9468	45.2176
10	75.9981	45.8640
15	69.2464	46.9205
20	62.7636	48.3589

Table 1. Values of ϕ and θ for varying α in degrees.

The polarization states at $\phi = 90^\circ$ are purely s- or p-polarization for the chief ray. When the deviation angle α increases the ellipticity becomes larger. The result could be that the contrast at the system becomes too low.

#6733 - $15.00 US
Received 1 March 2005; revised 14 March 2005; accepted 15 March 2005

6. Conclusions

An WGP made of aluminum reflects almost all of the visible light that is polarized such that the electric field is parallel to the wires and transmits almost all light of which the electric vector is perpendicular to the wires. We have explained this phenomenon by applying the theory of metallic waveguides. By applying a rigorous finite element model we have studied the sensitivity of the WGP for varying the period and the depth of the grooves. It was shown that for all visible wavelengths and for a sufficiently large range of conical incident angles, the WGP is very efficient. The results of the calculations have been compared with measurements and good agreement was obtained. We furthermore found that the effective medium method is a reasonable accurate method to study WGPs for LCoS systems.

Acknowledgments

The authors thank Stephen McClain for helpful discussions and providing the Moxtek samples. Furthermore Ms. M. Vervest is acknowledged for providing the SEM images.

#6733 - $15.00 US Received 1 March 2005; revised 14 March 2005; accepted 15 March 2005